Improving object density determination in coherent diffraction imaging by preprocessing truncated discrete diffraction amplitudes: supplemental document

1 Diffraction patterns used in simulations

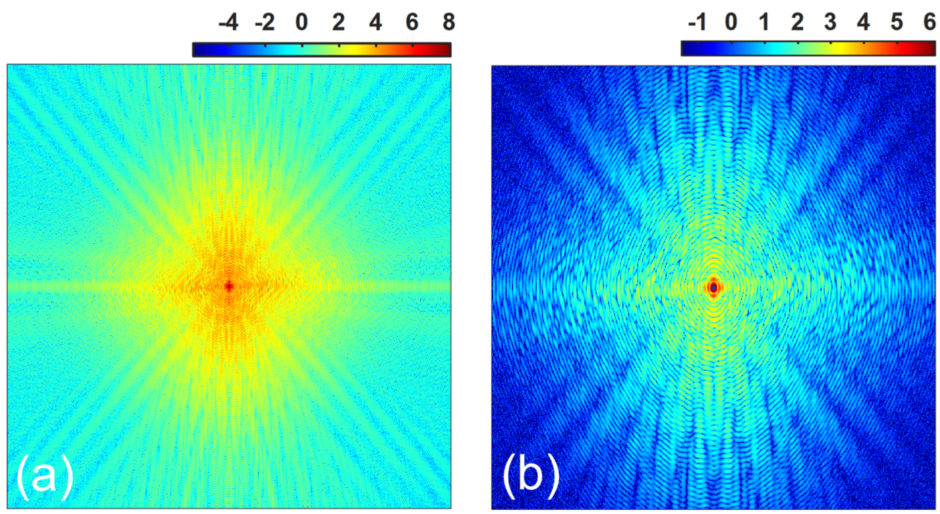

Figure S1: (a) Noiseless full diffraction intensity of the mitochondrion model density. (b) Noise added full diffraction intensity. The q range of (b) is half of that in (a).

2 Simulations for the origin of the artifacts

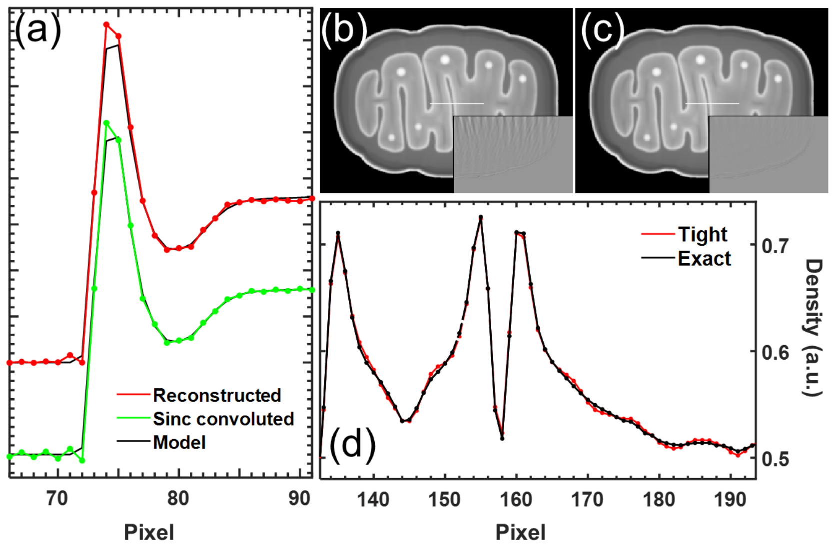

Figure S2: (a) Line profile of the reconstructed density shown in Fig. 1(g) in manuscript shown by the red line with the model density in the black lines. The green line is the sinc function convoluted $\rho(x)$ (down shifted by 0.2). Their similarity indicates that the artifact in the reconstructed density was caused by the truncation of diffraction intensity. (b, c) Reconstructed images obtained using the aliased diffraction pattern with a tight support (b) and an exact support (c). The tight support is $\sim$1 pixel smaller than the exact support. The aliased diffraction pattern yield superior reconstruction than the raw diffraction pattern. Insets in (b,c) are the difference images to the ground truth density, $\rho_{ave}(x)$. (d) Line profiles of from the (b,c) indicated by white lines.

As shown in Fig. S2(a), the Gibbs ring-like artifact in the reconstructed image much resembles the actual Gibbs ring shown in the sinc function convoluted density. Figure S2(b, c) show the aligned (best 50) images reconstructed using the ideal aliased $S(q)$ with the tight support and the exact support. There were no visible Gibbs ring-like artifacts in this case.

Images from the exact support are reconstructed near ideally. Meanwhile, small long ranged artifacts were observable from the tight support. Small intensities at the surface of the outer membrane is pushed to zero with this tight support. This contradicts with the Fourier constraint, and causes the long ranged artifacts. When the raw diffraction data is used, the obtained density is convoluted by a sinc function resulting Gibbs ring tail which spills out of the exact support. Similarly, this can be the source of the long-ranged artifacts.

3 Suppressing of the ringing pattern by a 'unring' method

In order to separate out the Gibbs phenomenon from the ringing artifacts, we suppressed them using a reported 'unring' method[2]. The following figures are the difference images after applying the method on each case.

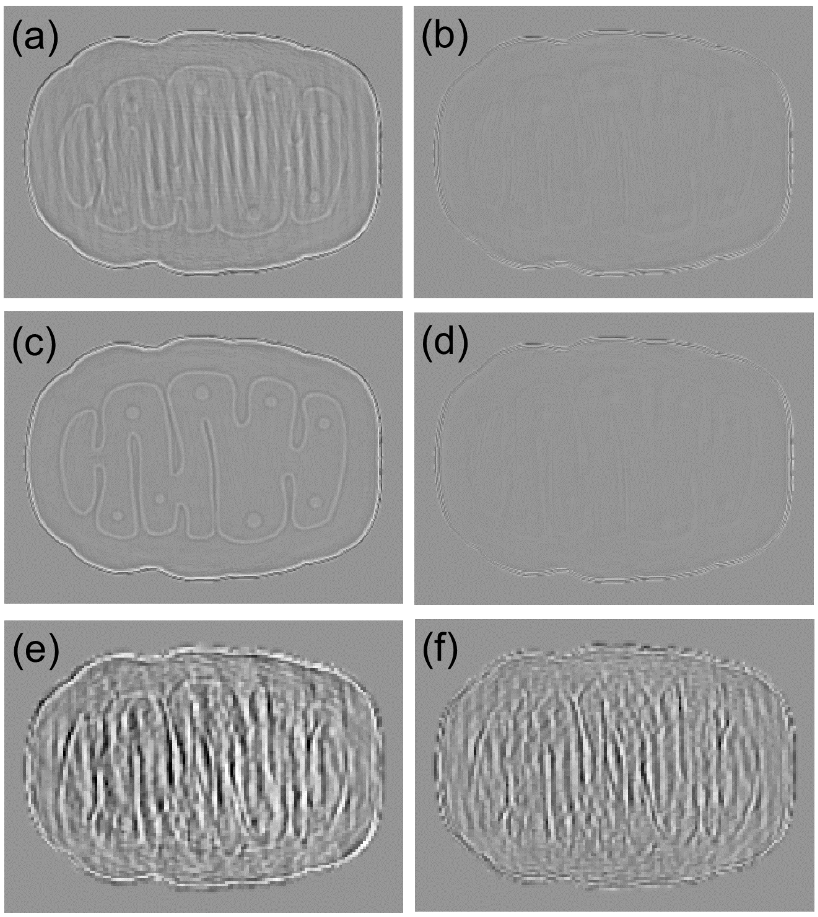

Figure S3: Difference images between the model density and the reconstructed density using Noiseless raw amplitude (a), Noiseless corrected(b), Noiseless raw with exclusion (c), Noiseless corrected with exclusion (d), Noise added raw (e), Noise added corrected with exclusion (f).

4 Number of excluded constraints

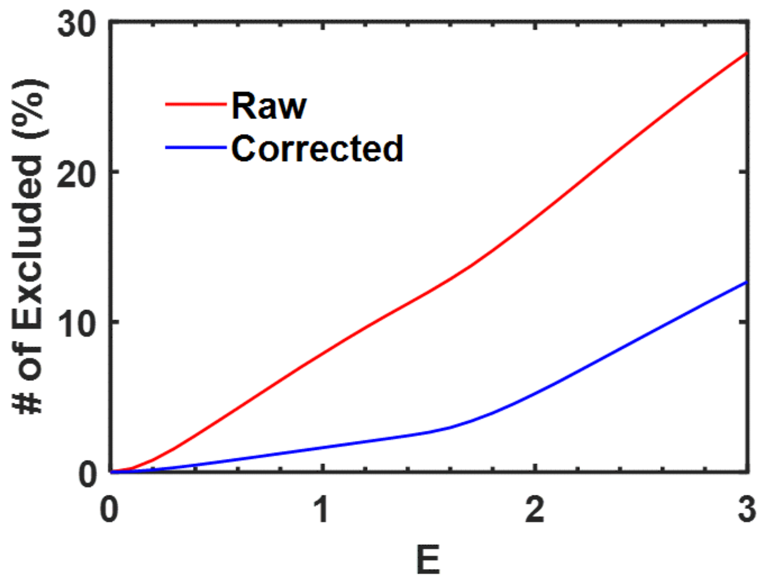

Figure S4: Number of excluded constraints versus E.

5 PRTFs

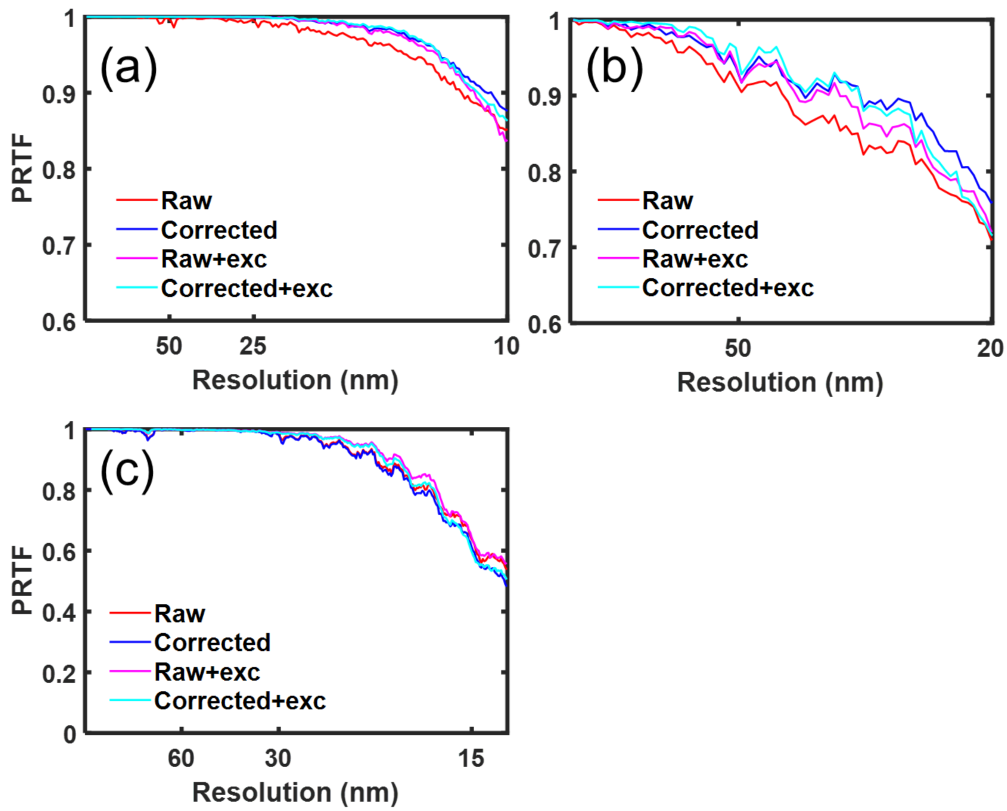

Figure S5: (a) PRTFs from the simulations using noiseless diffraction data. (b) PRTFs from noise added diffraction data. (c) PRTFs from mitochondrion/Au experimental data. The term '+exc' on legend refers Fourier constraint exclusion.

6 Results from the simulated data with the photon-shot noise

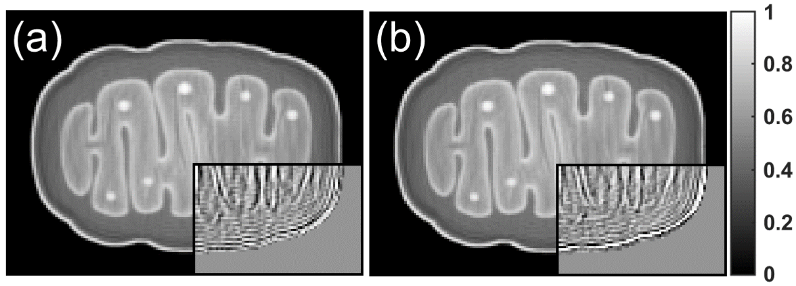

Figure S6: Reconstructed images from $|S_c(q_n)|$ (a), and $|S(q_n)|$ (b) with the exclusion of Fourier constraints. Insets show the deviation of the reconstructed images from the mitochondrion model density. The result from $|S_c(q_n)|$ with the exclusion is presented in the main manuscript.

7 Results from experimental data

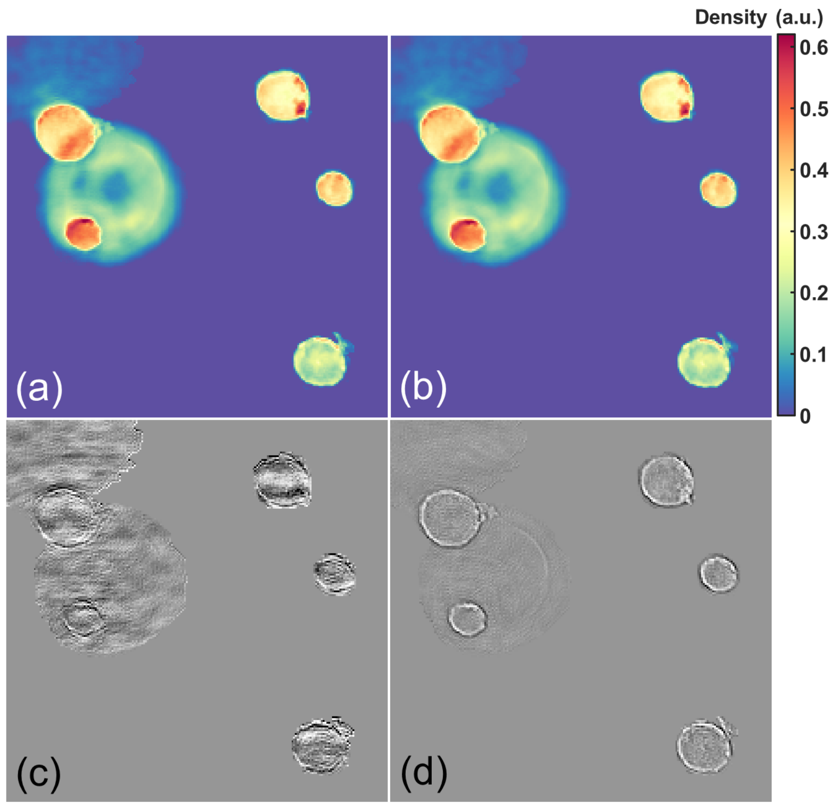

Figure S7: (a) Reconstructed image from the diffraction amplitude only multiplied by the correction factor. (b) Reconstructed image from the raw diffraction amplitudes with Fourier constraint exclusion only. In the main manuscript, we presented the case where both the correction and exclusion were applied. (c, d) Entire difference images obtained by subtracting correction and exclusion applied image from correction only and exclusion only image, respectively. Images are aligned before subtraction.

8 Effect of the correction factor for various OSRs

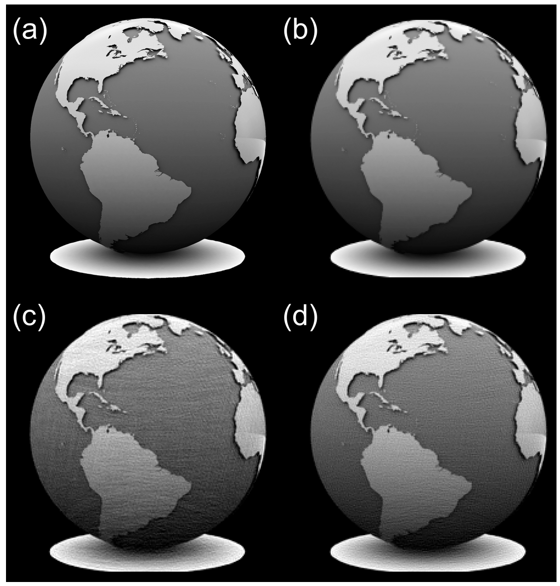

Figure S8: (a) 5000×3750 vector image of the globe cropped to 3248×2948, created by Madmaxer [1]. (b) GT image binned from globe image. Best reconstructed images from the raw (c) and correction factor multiplied (d). Fourier amplitudes are at the OSR of 2.8 in 2D.

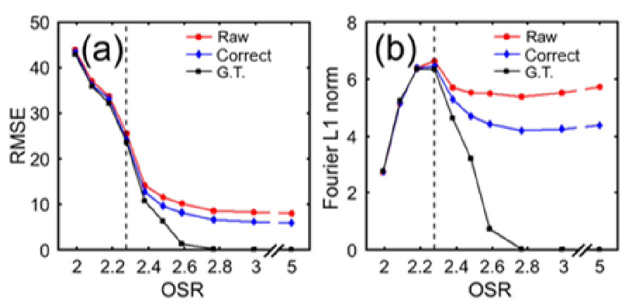

Figure S9: Analysis on reconstructed results of the globe image. (a, b) Unnormalized error indices of reconstructed globe images using RMSE (a) and Fourier L1 norm (b) at low OSRs.

References

[1] Madmaxer, Earth. url = 'https://www.dreamstime.com/earth-stock-photography-image-free-8541062'. Date of access : July 24th, 2023

[2] Kellner. et al (2016). *Gibbs-ringing artifact removal based on local subvoxel-shifts*. 1574-1581. 10.1002/mrm.26054